

# Computer Assembly of Cluster-Forming Amphiphilic Dendrimers

Bianca M. Mladek,<sup>1</sup> Gerhard Kahl,<sup>1</sup> and Christos N. Likos<sup>2</sup>

<sup>1</sup>Center for Computational Materials Science and Institut für Theoretische Physik,  
Technische Universität Wien, Wiedner Hauptstraße 8-10, A-1040 Wien, Austria

<sup>2</sup>Institut für Theoretische Physik II: Weiche Materie,  
Heinrich-Heine-Universität Düsseldorf, Universitätsstraße 1, D-40225 Düsseldorf, Germany  
(Dated: November 20, 2018)

Recent theoretical studies have predicted a new clustering mechanism for soft matter particles that interact via a certain kind of purely repulsive, bounded potentials. At sufficiently high densities, clusters of overlapping particles are formed in the fluid, which upon further compression crystallize into cubic lattices with density-independent lattice constants. In this work we show that amphiphilic dendrimers are suitable colloids for the experimental realization of this phenomenon. Thereby, we pave the way for the synthesis of such macromolecules, which form the basis for a novel class of materials with unusual properties.

PACS numbers: 82.70.Dd, 61.20.Ja, 64.75.Yz, 81.05.Zx

Self-assembly is the key-expression that circumscribes the incredibly rich wealth of ordered phases encountered in soft matter systems. Starting from the face-center cubic arrangement assumed by colloidal spheres at high concentrations [1, 2, 3] and low-symmetry crystals formed by soft spheres [4], they extend over to a variety of alloys seen for charged colloidal mixtures [5] and to the gyroid phases assembled in block copolymer solutions [6, 7, 8]. Recent theoretical and computational advances have predicted a novel form of self-assembly in soft matter, i.e., the formation of stable clusters [9, 10] encountered for *purely repulsive*, bounded effective potentials  $\Phi_{\text{eff}}(r)$ . These clusters crystallize into cubic lattices at sufficiently high densities and all temperatures [9, 10]. This phenomenon bears significant consequences both from the fundamental point of view [10] and from the aspect of the properties of the ensuing materials, e.g., their diffusion and relaxation dynamics [11]. Though thoroughly understood at the level of effective potentials, the phenomenon begs the question: *What kinds of particles display the class of effective interactions giving rise to this phase behavior?* In this contribution we demonstrate that relatively simple macromolecules can be designed to achieve this aim, taking advantage of the great flexibility offered by soft matter systems to manufacture new materials.

The underlying theoretical concepts can be clearly stated as follows. Repulsion-induced aggregation which leads to ordered cluster phases requires that the Fourier transform (FT)  $\tilde{\Phi}_{\text{eff}}(k)$  of  $\Phi_{\text{eff}}(r)$  has negative parts for some values of the wave-vector  $k$ . If, however,  $\tilde{\Phi}_{\text{eff}}(k) > 0$  for all  $k$ , reentrant melting occurs instead [12]. A sufficient condition for the former is that  $\Phi_{\text{eff}}''(r=0) \geq 0$  [10]. Useful archetypes of bounded interactions [9, 10] are the generalized exponential models of index  $n$  (GEM- $n$ ), where  $\Phi_n(r) = \varepsilon \exp[-(r/\sigma)^n]$ , with  $\varepsilon$  and  $\sigma$  being some energy- and length-scales: here, for  $n > 2$  clustering takes place, whereas for  $n \leq 2$  reentrant melting occurs [13].

Searching for realizations of clustering-type potentials, we concentrate on dendrimers, a choice motivated by

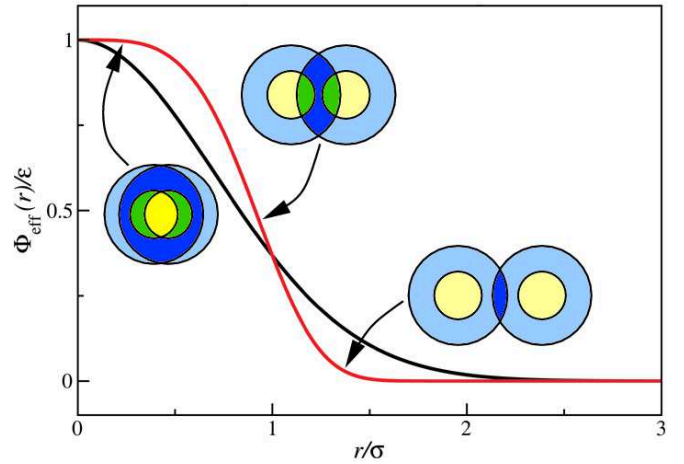


FIG. 1: (Color online) Schematic representation of the effective potentials of amphiphilic dendrimers: interactions between the different regions (solvophobic core - yellow, solvophilic shell - blue) of amphiphilic dendrimers lead to interactions that are steeper (red line) than the threshold of clustering (Gaussian, black line).

their outstanding properties. They are characterized by a high degree of monodispersity and a well-defined, highly branched internal structure; efficient dendrimer assembly has been boosted by recent progress in synthetic techniques [14]. Fundamentally, they serve as tunable soft colloids that allow for control of their effective interactions via changes in chemical composition, bond length and generation number [15, 16]. For athermal dendrimers,  $\Phi_{\text{eff}}(r)$  has a Gaussian shape [15] ( $n = 2$  in the GEM- $n$  family), hinting thus to the reentrant melting scenario. Closely linked with these findings is the dense-core structure of these dendrimers, arising from back-folding of the terminal groups [16, 17].

Following the ideas of material design, we modify the architecture of athermal, flexible dendrimers along well-

defined strategies. Since the Gaussian effective interaction is at the threshold to clustering, we require the following changes in  $\Phi_{\text{eff}}(r)$  to achieve clustering behavior: a flatter core region, such as those of the GEM- $n$  potentials with  $n > 2$ , which – compared to a Gaussian – also display a steeper decay of the repulsion for larger separations. Alternatively, a positive effective interaction with a local *minimum* at  $r = 0$  also leads to oscillations in  $\hat{\Phi}_{\text{eff}}(q)$ , as we have  $\Phi_{\text{eff}}''(r = 0) > 0$  in that case. To realize this goal, we aim for a more open structure and stronger segregation between outer and inner particles by assembling *amphiphilic* dendrimers built up from a solvophilic shell and solvophobic core particles. In Fig. 1, we qualitatively illustrate how our modifications lead in the correct direction: as the macromolecules start to overlap, the solvophilic and thus mutually repulsive shells cause a steeply increasing potential wall. This effect is reinforced upon further decreasing the distance since core and shell repel each other due to their different nature. Eventually, the attractive core regions overlap and slow down further growth of the repulsion, leading to a rather flat region or even a local minimum in  $\Phi_{\text{eff}}(r)$  at small distances.

In an effort to realize these ideas we developed a computer model of second generation [16] amphiphilic dendrimers [18] where the end-groups form the solvophilic shell (index S) and all other monomers the solvophobic core (index C). The bonds between monomers are modeled by the finitely extensible nonlinear elastic (FENE) potential [19]

$$\beta\Phi_{\mu\nu}^{\text{FENE}}(r) = -K_{\mu\nu}R_{\mu\nu}^2 \log \left[ 1 - \left( \frac{r - l_{\mu\nu}^0}{R_{\mu\nu}} \right)^2 \right], \quad (1)$$

with  $\mu\nu = \text{CC}, \text{CS}$ , which restricts the bond-length to be in between  $l_{\mu\nu}^{\text{max}}$  and  $l_{\mu\nu}^{\text{min}}$ .  $K_{\mu\nu}$  is the spring-constant and  $R_{\mu\nu} = l_{\mu\nu}^{\text{max}} - l_{\mu\nu}^0$ , with  $l_{\mu\nu}^0 = (l_{\mu\nu}^{\text{max}} + l_{\mu\nu}^{\text{min}})/2$  being the equilibrium bond length. All other interactions between two monomers separated by distance  $r$  are modeled by the Morse potential

$$\beta\Phi_{\mu\nu}^{\text{Morse}}(r) = \varepsilon_{\mu\nu} \left\{ \left[ e^{-\alpha_{\mu\nu}(r-d_{\mu\nu})} - 1 \right]^2 - 1 \right\}, \quad (2)$$

with  $\mu\nu = \text{CC}, \text{CS}, \text{SS}$ , which is characterized by a repulsive core at short and an attractive tail at long distances whose depth and range are parametrized by  $\varepsilon_{\mu\nu}$  and  $\alpha_{\mu\nu}$ , respectively. The  $d_{\mu\nu}$  are the monomer diameters. All potential parameters of the dendrimers discussed in this work are summarized in Table I.

We calculated the monomer density profiles for the core and the shell particles,  $\rho_C(r)$  and  $\rho_S(r)$ , in standard Monte Carlo (MC) simulations of an *isolated* dendrimer. Representative results pertaining to two ( $D_1, D_2$ ) out of seven model dendrimers simulated are shown in Fig. 2. They demonstrate that both the core- and the shell-particle distributions are of Gaussian shape, with the fitting parameters given in the respective panels. In striking contrast to athermal dendrimers (see Fig.

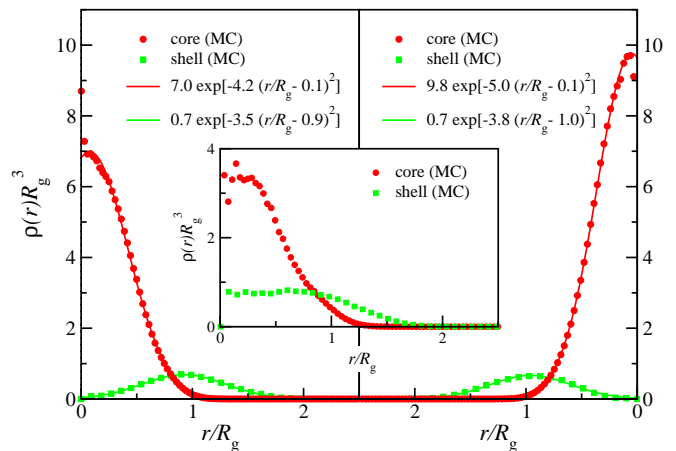


FIG. 2: (Color online) Monomer density profiles of the core (red) and the shell (green) region as obtained by MC simulations (symbols) and from fits to Gaussians (lines) for the amphiphilic dendrimers  $D_1$  (left panel) and  $D_2$  (right panel). The interaction parameters are given in Table I. In the inset, we show the same for an athermal dendrimer of the same generation.

<b>FENE</b>	$K/d_{\text{CC}}^2$	$l_0/d_{\text{CC}}$	$R/d_{\text{CC}}$
CC	40	1.875	0.375
CS	20	3.750	0.750
ZZ	40	2.8125 ( $D_1$ )	0.5625 ( $D_1$ )
		1.8750 ( $D_2$ )	0.3750 ( $D_2$ )
<b>Morse</b>	$\varepsilon$	$\alpha d_{\text{CC}}$	$d/d_{\text{CC}}$
CC	0.714	6.4	1
CS	0.014	19.2	1.50 ( $D_1$ )
			1.25 ( $D_2$ )
SS	0.014	19.2	2.0 ( $D_1$ )
			1.5 ( $D_2$ )

TABLE I: Potential parameters of the dendrimers considered in this study [cf. Eqs. (1) and (2)], labeled  $D_1$  and  $D_2$ . ZZ refers to the two central monomers.

2, inset), these density profiles are – due to amphiphilicity – spatially segregated: the distribution of the core monomers has its maximum close to the origin while the profile of the shell particles is centered between  $0.85 R_g$  and  $R_g$  (for all seven dendrimers simulated), with  $R_g$  being the dendrimer’s radius of gyration.

Next, we performed MC simulations between two interacting dendrimers, averaging over the degrees of freedom of the constituent monomers to determine the effective potential,  $\Phi_{\text{eff}}(r)$ . Allowing two dendrimers to interact freely, their effective potential can be determined from the centers-of-mass (c.o.m.) correlation function  $G(r)$ , given by  $G(|\mathbf{R}_1 - \mathbf{R}_2|) = \langle \hat{\rho}_1(\mathbf{R}_1) \hat{\rho}_2(\mathbf{R}_2) \rangle$ . Here,  $\hat{\rho}_i(\mathbf{R}_i) = \delta(\mathbf{R}_i - \mathbf{S}_i)$  is the density operator for the c.o.m. of dendrimer  $i$ , and the average  $\langle \dots \rangle$  is taken over all c.o.m. position vectors  $\mathbf{S}_i$  ( $i = 1, 2$ ).  $\Phi_{\text{eff}}(r)$  is

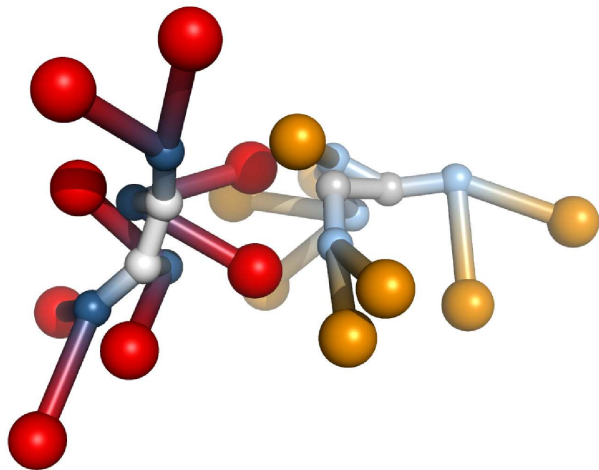


FIG. 3: (Color online) Simulation snapshot of two interacting amphiphilic dendrimers, both showing a dense shell conformation.

then given by  $\beta\Phi_{\text{eff}}(r) = -\ln[G(r)]$ , with  $\beta = 1/k_{\text{B}}T$ . Since the repulsion between the dendrimers is expected to be strong at short distances, this scheme will provide only poor statistics for small separations. To cope with this problem, we use non-Boltzmann sampling [20] where we divide the  $r$ -range into  $m = 15$  windows of width  $\Delta r_j = \frac{2r_{\text{max}}}{m(m+1)}(j+1)$  and assume for each window  $j = 0, \dots, m-1$  an umbrella potential  $W_j(r)$ :

$$W_j(r) = \begin{cases} 0 & r_j - \delta r < r < r_j + \Delta r_j + \delta r \\ \infty & \text{else} \end{cases} \quad (3)$$

Here,  $r_0 = 0$  and else  $r_j = \sum_{i=0}^{j-1} \Delta r_i$ . Further,  $r_{\text{max}} = 5R_g$  and  $\delta r$  is chosen to guarantee for slightly overlapping windows (at the edges,  $\delta r = 0$ .) For each of these windows, simulations of  $2 \times 10^8$  MC sweeps are performed and  $G_j(r)$  is determined to within an additive constant due to normalization. We obtain  $\Phi_{\text{eff},j}(r)$  in each window  $j$  as  $-k_{\text{B}}T \ln G_j(r)$  and these results are merged to form a continuous curve which is finally normalized by setting  $\beta\Phi_{\text{eff}}(r = r_{\text{max}}) = 0$ .

A typical simulation snapshot of two interacting dendrimers is shown in Fig. 3. Results for the effective interactions of the two dendrimers are summarized in Fig. 4.  $\Phi_{\text{eff}}(r)$  indeed shows a steep increase as the macromolecules approach and eventually becomes rather flat [Fig. 4(a)], or even exhibits a locally attractive dip [Fig. 4(c)] for smaller distances. We fitted  $\Phi_{\text{eff}}(r)$  of dendrimer  $D_1$  by a GEM- $n$  potential, finding that  $\Phi_n(r)$  with an index  $n \cong 3.1$  approximates it with high accuracy. The effective potential of dendrimer  $D_2$  can be fitted to a double-Gauss of the form  $\Phi_{\text{eff}}(r) = \epsilon_1 \exp[-(r/\sigma_1)^2] - \epsilon_2 \exp[-(r/\sigma_2)^2]$ , where  $\epsilon_1 = 23.6k_{\text{B}}T$ ,  $\epsilon_2 = 22.5k_{\text{B}}T$ ,  $\sigma_1 = 1.117R_g$  and  $\sigma_2 = 1.059R_g$ . Both effective potentials lead to clustering, since  $\Phi_{\text{eff}}'(r = 0) \geq 0$ .

To provide a semi-quantitative theoretical background

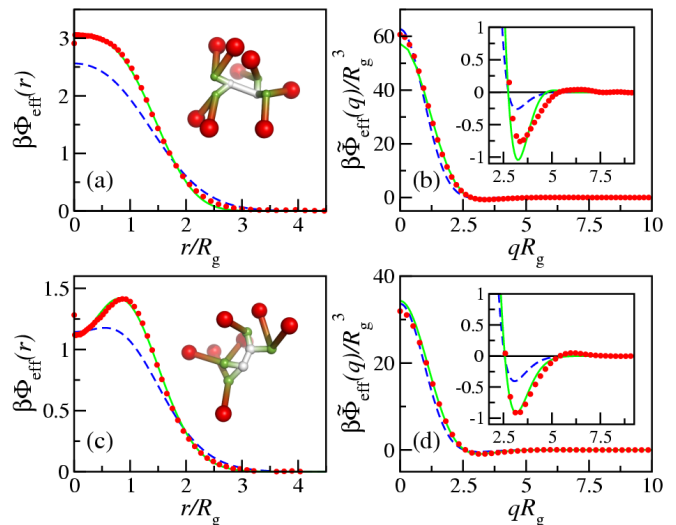


FIG. 4: (Color online) The effective potentials  $\Phi_{\text{eff}}(r)$  of typical amphiphilic dendrimers [(a), (c)] and their FTs  $\tilde{\Phi}_{\text{eff}}(q)$  [(b), (d)], showing negative parts. The blue dashed line denotes the theoretical result (see text), and the green lines are fits to the simulation data. (a) and (b) pertain to dendrimer  $D_1$ , (c) and (d) to  $D_2$ . The insets in (a) and (c) feature simulation snapshots of the respective dendrimers.

to these simulation results, we reconsider our amphiphilic dendrimers within a suitably modified Flory theory. The original idea of this concept [21] is based on the simplifying assumptions that the spherically symmetric monomer densities of isolated athermal dendrimers around the c.o.m.,  $\rho(r)$ , do not change upon close interaction. Here,  $\rho(r) = \langle \sum_j \delta(\mathbf{r} - \mathbf{r}_j) \rangle$  and  $\mathbf{r}_j$  denotes the position vector of monomer  $j$  with respect to the center of mass. Thus, considering two such dendrimers at separation  $\mathbf{R}$  and *assuming* that their profiles are not distorted by their mutual presence, the effective interaction between the two dendrimers takes the form

$$\Phi_{\text{eff}}(|\mathbf{R}|) = \iint \rho(|\mathbf{r}_1|)\rho(|\mathbf{r}_2 - \mathbf{R}|)v(|\mathbf{r}_1 - \mathbf{r}_2|)d\mathbf{r}_1d\mathbf{r}_2, \quad (4)$$

where  $v(|\mathbf{r}_1 - \mathbf{r}_2|)$  is the monomer-monomer interaction. For the latter, a contact interaction weighted by the second virial coefficient  $v_0$  of the monomer-monomer interaction is introduced,  $\beta v(|\mathbf{r}_1 - \mathbf{r}_2|) = v_0\delta(|\mathbf{r}_1 - \mathbf{r}_2|)$ . For athermal dendrimers,  $v_0 > 0$ . The FT of  $\Phi_{\text{eff}}(r)$  given in Eq. (4) then reads in this case  $\beta\tilde{\Phi}_{\text{eff}}(k) = v_0\tilde{\rho}^2(k) > 0 \forall k$ .

Generalizing this model to amphiphilic dendrimers, we treat the core and the shell profiles separately, introducing *three* different excluded volume parameters,  $v_{\text{CC}}$ ,  $v_{\text{CS}}$ , and  $v_{\text{SS}}$  given by the second virial coefficients of the underlying monomer-monomer interactions. Proceeding along similar lines as above leads to the FT of the effective interaction between amphiphilic dendrimers as  $\beta\tilde{\Phi}_{\text{eff}}(k) = \sum_{\mu,\nu} v_{\mu\nu}\tilde{\rho}_\mu(k)\tilde{\rho}_\nu(k)$  where  $\tilde{\rho}_\mu(k)$  is the FT of  $\rho_\mu(r)$  and  $\mu, \nu = \text{C, S}$ . Core solvophobicity implies  $v_{\text{CC}} < 0$ , whereas  $v_{\text{CS}}, v_{\text{SS}} > 0$ . Consequently,

$\tilde{\Phi}_{\text{eff}}(k)$  can also display negative components. The values of the second virial coefficients for our dendrimers are  $v_{\text{CC}} = -1.90$ ,  $v_{\text{SS}} = 28.40$  and  $v_{\text{CS}} = 11.31$  ( $D_1$ ), and  $v_{\text{CC}} = -1.90$ ,  $v_{\text{SS}} = 11.31$  and  $v_{\text{CS}} = 6.25$  ( $D_2$ ), measured in  $d_{\text{CC}}^{-3}$ . Based on the simulation results (cf. Fig. 2), we model the monomer densities  $\rho_\mu(r)$  as Gaussian functions,  $\rho_\mu(r) = S_\mu \exp[-\gamma_\mu(r - r_\mu)^2]$ , taking for  $S_\mu$ ,  $\gamma_\mu$ , and  $r_\mu$ ,  $\mu = \text{C, S}$ , those values that provide the best fit of the simulation data, quoted in Fig. 2. Approximate expressions for the  $\tilde{\rho}_\mu(k)$  are given in [22]. The theoretical results for  $\tilde{\Phi}_{\text{eff}}(k)$  and hence  $\Phi_{\text{eff}}(r)$  are shown in Fig. 4 along with the data extracted from the simulations. In view of the simplifying assumptions of Flory theory, the good qualitative agreement between simulations and theory is astonishing. The negative Fourier components [Figs. 4(b) and 4(d)], are less pronounced in theory than in simulation, thus the former provides a lower threshold to the onset of clustering.

The counterintuitive phenomenon of clustering in the complete absence of attraction might motivate experimental groups to assemble amphiphilic dendrimers in the lab. To this end let us summarize our guidelines for synthesizing clustering dendrimers. In a first step, suitable solvophobic core and solvophilic shell groups have to be chosen for the experiments, for which simulations on an isolated dendrimer are performed, leading to the core- and the shell-density profiles. While Flory theory provides a reliable qualitative indicator whether the threshold to clustering has already been reached, full evidence can then be gathered by measuring the effective interactions in the more time-consuming simulations of two interacting dendrimers. From our observations for all dendrimers investigated, the following remarks should prove valuable: bigger end-groups and/or shorter end-

group spacers lead to a stronger repulsion in  $\Phi_{\text{eff}}(r)$  at short distances. Further, if the spacer length of the end-groups is increased and/or the distance between the two central particles and/or the end-group particle size is reduced,  $\Phi_{\text{eff}}(r)$  becomes flatter or even develops a dip at small distances. The low dendrimer-generation number is encouraging for experimentalists because it hints at a rather straightforward synthesis process [14]. Since  $\Phi_{\text{eff}}(r = 0) \sim k_{\text{B}}T$ , clustering can easily be realized under ambient conditions in thermally activated processes.

The findings of this work bear significance for soft matter science and materials design at various levels. At the one-particle level, we have established that synthesizing open dendrimers with a segregated core-shell structure requires neither stiff bonds nor electrostatic repulsions as commonly believed: amphiphilicity is sufficient. At the many-body level, solutions of such dendrimers will display pronounced correlations at a *single* length scale, independently of the density [10], allowing thus for well-controlled spatial modulation of confined liquids and, e.g., their local index of refraction, whose intensity can be tuned by changing the degree of confinement. Crystals formed by such systems show density-*independent* lattice constants, a novel of self-assembly of condensed matter. Such crystals are quite unusual, since they are diffusive on the single-particle level, allowing thus mass transport but arrested, and thus rigid as a conventional solid, at the collective level [11]. Finally, on the fundamental level, we have demonstrated that within soft matter, bounded effective interactions can be manipulated with the same degree of flexibility as diverging ones do.

We thank D. Gottwald for helpful discussions. This work was funded by the FWF, Proj. No. 17823-N08 and by the DFG within the SFB-TR6, Project Section C3.

- 
- [1] P. N. Pusey and W. van Meegen, *Nature* **320**, 340 (1986).  
 [2] U. Gasser, E. R. Weeks, A. Schofield, P. N. Pusey, and D. A. Weitz, *Science* **292**, 258 (2001).  
 [3] V. J. Anderson and H. N. W. Lekkerkerker, *Nature* **416**, 811 (2002).  
 [4] P. Ziherl and R. D. Kamien, *Phys. Rev. Lett.* **85**, 3528 (2000).  
 [5] M. E. Leunissen, C. G. Christova, A. P. Hynninen, C. P. Royall, A. I. Campbell, A. Imhof, M. Dijkstra, R. van Roij, and A. van Blaaderen, *Nature* **437**, 235 (2005).  
 [6] D. A. Hajduk, P. E. Harper, S. M. Gruner, C. C. Honeker, G. Kim, E. L. Thomas, and L. J. Fetters, *Macromolecules* **27**, 4063 (1994).  
 [7] W. M. Matsen, *J. Chem. Phys.* **108**, 785 (1998).  
 [8] C. K. Ullal, M. Maldovan, E. L. Thomas, G. Chen, Y. J. Han, and S. Yang, *Appl. Phys. Lett.* **84**, 5434 (2004).  
 [9] B. M. Mladek, D. Gottwald, G. Kahl, M. Neumann, and C. N. Likos, *Phys. Rev. Lett.* **96**, 045701 (2006).  
 [10] C. N. Likos, B. M. Mladek, D. Gottwald, and G. Kahl, *J. Chem. Phys.* **126**, 224502 (2007).  
 [11] A. J. Moreno and C. N. Likos, *Phys. Rev. Lett.* **99**, in press (2007).  
 [12] C. N. Likos, A. Lang, M. Watzlawek, and H. Löwen, *Phys. Rev. E* **63**, 031206 (2001).  
 [13] A. Lang, C. N. Likos, M. Watzlawek, and H. Löwen, *J. Phys.: Condens. Matter* **12**, 5087 (2000).  
 [14] P. Antoni, D. Nyström, C. J. Hawker, A. Hult, and M. Malkoch, *Chem. Commun.* 2249 (2007).  
 [15] I. O. Götze, H. M. Harreis, and C. N. Likos, *J. Chem. Phys.* **120**, 7761 (2004).  
 [16] M. Ballauff and C. N. Likos, *Angew. Chem. Int. Ed.* **43**, 2998 (2004).  
 [17] T. C. Zook and G. T. Pickett, *Phys. Rev. Lett.* **90**, 015502 (2003).  
 [18] G. Giupponi and D. M. A. Buzza, *J. Chem. Phys.* **122**, 194903 (2005).  
 [19] G. S. Grest, K. Kremer, and T. A. Witten, *Macromolecules* **20**, 1376 (1987).  
 [20] D. Chandler, *Introduction to Modern Statistical Mechanics* (Oxford University Press, Oxford, 1987).  
 [21] M. Doi and S. F. Edwards, *The Theory of Polymer Dynamics* (Clarendon Press, Oxford, 1986).  
 [22] J.-P. Hansen and C. Pearson, *Mol. Phys.* **104**, 3389 (2007).